scientific reports

Check for updates

OPEN

Doublecortin-like knockdown in mice attenuates obesity by stimulating energy expenditure in adipose tissue

Melanie Modder[1], Claudia P. Coomans[2], Dirk-Jan Saaltink[2], Mayke M. H. Tersteeg[2], Janna Hoogduin[2], Leonie Scholten[2], Amanda C. M. Pronk[1], Reshma A. Lalai[1], Anita Boelen[3], Andries Kalsbeek[3,4,5], Patrick C. N. Rensen[1], Erno Vreugdenhil[2] & Sander Kooijman[1,6]✉

Crosstalk between peripheral metabolic organs and the central nervous system is essential for body weight control. At the base of the hypothalamus, β-tanycytes surround the portal capillaries and function as gatekeepers to facilitate transfer of substances from the circulation into the cerebrospinal fluid and vice versa. Here, we investigated the role of the neuroplasticity gene doublecortin-like (DCL), highly expressed by β-tanycytes, in body weight control and whole-body energy metabolism. We demonstrated that DCL-knockdown through a doxycycline-inducible shRNA expression system prevents body weight gain by reducing adiposity in mice. DCL-knockdown slightly increased whole-body energy expenditure possibly as a result of elevated circulating thyroid hormones. In white adipose tissue (WAT) triglyceride uptake was increased while the average adipocyte cell size was reduced. At histological level we observed clear signs of browning, and thus increased thermogenesis in WAT. We found no indications for stimulated thermogenesis in brown adipose tissue (BAT). Altogether, we demonstrate an important, though subtle, role of tanycytic DCL in body weight control through regulation of energy expenditure, and specifically WAT browning. Elucidating mechanisms underlying the role of DCL in regulating brain-peripheral crosstalk further might identify new treatment targets for obesity.

Keywords Doublecortin-like, β-Tanycytes, Body weight control, Energy expenditure, White adipose tissue browning

Obesity is a disease with a complex multifactorial pathogenesis that forms a growing worldwide health problem because of the many related comorbidities such as type 2 diabetes and cardiovascular diseases. Crosstalk between peripheral metabolic organs and the central nervous system is essential to keep energy homeostasis. As such, entrance of metabolites and hormones secreted by peripheral organs into the brain, and vice versa, is carefully regulated. Most vasculature in the brain is surrounded by a tight, non-permeable endothelium, known as the blood–brain barrier (BBB), and only peri- or circumventricular organs form an alternative semi-permeable barrier between the peripheral blood stream and the cerebrospinal fluid (CSF)[1].

An example of a circumventricular organ is the median eminence (ME), located at the bottom of the third ventricle, where hypothalamic neurons converge onto the portal vasculature of the anterior pituitary gland. Tanycytes reside in the ME and serve as gatekeepers for metabolites and hormones reaching the CSF and hypothalamic nuclei involved in regulating energy intake and energy expenditure[2–5]. Four subtypes of tanycytes have been described based on location and gene expression patterns: α1-, α2-, β1-, and β2-tanycytes. Structurally, tanycyte cell bodies line the third ventricle while their dynamic end-feet extend onto other structures,

[1]Division of Endocrinology, Department of Medicine, Leiden University Medical Center, P.O. Box 9600, 2300 RC Leiden, The Netherlands. [2]Laboratory for Neurophysiology, Department of Cell and Chemical Biology, Leiden University Medical Center, P.O. Box 9600, 2300 RC Leiden, The Netherlands. [3]Endocrine Laboratory, Amsterdam UMC, Location AMC, University of Amsterdam, Amsterdam, The Netherlands. [4]Department of Endocrinology and Metabolism, Amsterdam UMC, Location AMC, University of Amsterdam, Amsterdam, The Netherlands. [5]Hypothalamic Integration Mechanisms, Netherlands Institute for Neuroscience, Amsterdam, The Netherlands. [6]Leiden University Medical Center, Albinusdreef 2, 2333ZA Leiden, The Netherlands. ✉email: s.kooijman@lumc.nl

including hypothalamic nuclei in case of α1- and α2-tanycytes and portal capillaries of the ME in case of β1-, and β2-tanycytes.

β2-tanycytes are equipped with transport machinery to facilitate transfer of substances and are known to transfer amongst others leptin and glucose (derivatives) from the circulation into the CSF, making tanycytes essential for connecting these peripheral signals to hypothalamus[6–8]. In addition, tanycytes are thought to control activity of the hypothalamic–pituitary–thyroid axis (HPT-axis) by regulating the release of thyrotropin-releasing hormone (TRH) into pituitary capillaries[2,9,10]. Moreover, β2-tanycytes specifically express the triiodothyronine (T_3)-generating enzyme thyroxine deiodinase type 2 (D2), suggesting that these cells are key for the actions of T_3 in the brain[11–13].

In previous studies, we identified the neuroplasticity gene doublecortin-like (DCL), a splice-variant of DCL kinase-1 (DCLK-1), to be highly expressed by β-tanycytes in the ME[14]. DCL is a microtubule-associated protein that (de)stabilizes the microtubule cytoskeleton and thereby enables dynamic movement of a cell and/or trafficking of signaling molecules through the cell[15,16]. DCL has also been shown to be abundantly expressed in restricted brain regions characterized by high levels of neuronal plasticity[16,17]. Presently, the role of DCL in β2-tanycytes is still unknown. Based on the previously described role of tanycytes in metabolic homeostasis[5,18–20], we hypothesized that tanycytic DCL may be important for energy balance by regulation of body weight control, adipose tissue and thyroid hormone production. For that reason, in the present study we investigated how energy metabolism and body weight control are altered in DCL knockdown (DCL-KD) mice.

Results

DCL-KD attenuates body weight and fat mass gain

We set out to evaluate the function of DCL expression by β-tanycytes in regulating whole-body energy metabolism by studying the phenotype of DCL-KD mice for which we made use of a doxycycline (dox)-inducible shRNA expression system. First, knockdown of DCL in the mediobasal hypothalamus was confirmed after five weeks of dox-containing diet (Fig. 1A–D). In line with our previous findings[14], wildtype (WT) littermates showed clear DCL expression both in dendrites and cell bodies of hypothalamic β-tanycytes present in the lower part of the third ventricle wall close to the ME (Fig. 1A,C). In contrast, DCL-KD mice had strongly reduced DCL

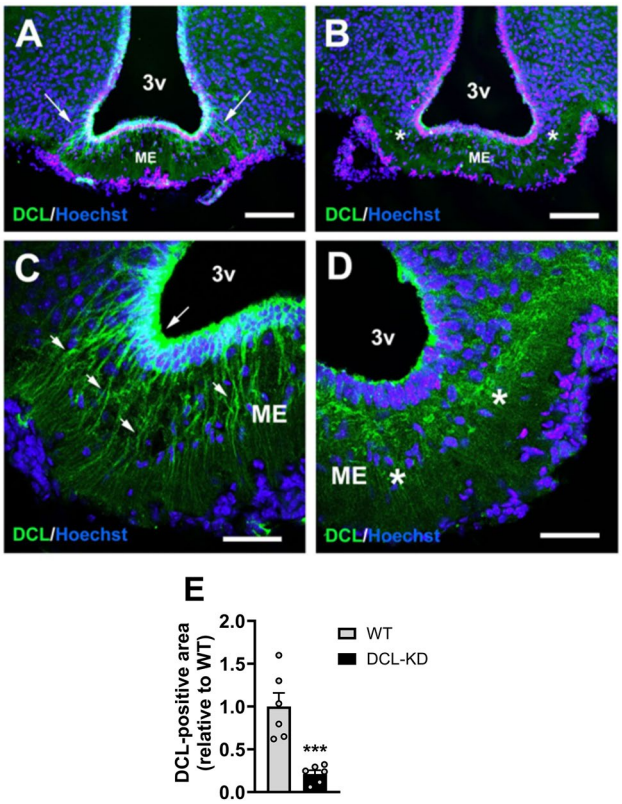

Fig. 1. Confirmation of DCL knockdown in β-tanycytes lining the median eminence. DCL-KD mice and WT littermates were put on a dox-containing diet for 5 weeks to induce DCL knockdown in the transgenic mice. Confocal microscopy was performed in the hypothalamus of (**A**,**C**) WT and (**B**,**D**) DCL-KD mice to show and quantify (**E**) DCL expression (green) in the wall of the third ventricle (3v) (n = 6 per group). Arrows indicate DCL positive projections into median eminence (ME). Asterisks indicate areas of clearly reduced DCL expression. Scale bars measure 100 µm in (**A**) and (**B**), and 40 µm in (**C**) and (**D**). Data is presented as mean ± SEM. ***P < 0.001 according to unpaired t-test (**E**).

expression in tanycyte dendrites and only a weak signal in the ventricle wall (Fig. 1B,D). Quantification of the immunohistochemical images suggested a 80% knockdown efficiency (Fig. 1E), which is in line with efficacy previously determined by immunohistochemistry and Western blot analysis in other nuclei[17,21].

We continued by assessing the effect of DCL-KD on body composition in a long-term study. At baseline, body mass, fat mass, and lean mass were similar between DCL-KD mice and WT littermates (Fig. 2A–C). In contrast, after 6 weeks of dox-containing diet, body mass of DCL-KD mice was lower than that of WT littermates (Fig. 2A), explained by a reduction in fat mass (Fig. 2B), while lean mass was not different between genotypes (Fig. 2C). The difference in body weight between DCL-KD and WT mice reached 10 g after 32 weeks of dox-containing diet (Fig. 2A), equivalent to a 23.7% lower body weight in DCL-KD mice compared to WT mice. After switching the dox-containing diet back to a dox-free diet, body weight normalized and was no longer different between DCL-KD and WT mice at week 52 (Fig. 2A).

To assess whether the reduced fat mass accumulation in DCL knockdown animals was caused by lower energy intake and/or increased energy expenditure, mice were temporarily individually housed in metabolic home cages to study these factors by means of indirect calorimetry during the first 4 days of dox-containing diet. Food intake did not differ between the genotypes (Fig. 2D), suggesting that energy expenditure must be increased. DCL-KD showed slightly elevated energy expenditure compared with WT mice, as indicated by the two-way ANOVA genotype effect and only when expressed per gram lean mass (Fig. 2E; uncorrected data Supplementary Fig. S1A; corresponding VO_2 and VCO_2 data Supplementary Fig. S1B–E). More specifically, we found an elevated fat oxidation rate in the light phase (Fig. 2F; uncorrected data Supplementary Fig. S1F) while the carbohydrate oxidation rate was similar between DCL-KD and WT mice (Fig. 2G; uncorrected data Supplementary Fig. S1G), as was the respiratory exchange ratio (Supplementary Fig S1H,I). Linear regression analysis suggested elevated energy expenditure independent of changes in lean mass (Fig. 2H,I) or body weight (Supplementary Fig. S1I,J).

DCL-KD increases serum thyroid hormone levels

Tanycytes control the activity of the HPT-axis and thyroid hormones are important regulators of basal metabolic rate[2,22]. We therefore analyzed if DCL-KD altered thyroid hormone levels in serum of fed mice and after prolonged fasting, as nutritional state also greatly affects activity of the HPT-axis. DCL-KD slightly, but significantly, increased serum thyroxine (T_4) levels independent of nutritional state (Fig. 2J), as indicated by the two-way ANOVA genotype effect. At tissue level, relatively inactive T_4 can be converted into active T_3 by deiodinase enzymes. T_3 serum levels were also increased in DCL-KD mice compared with WT littermates (Fig. 2K). Interestingly, in DCL-KD mice we also found raised hypothalamic D2 activity, in particular in the ad libitum fed state (Fig. 2L), which was somewhat unexpected because elevated thyroid hormone levels typically attenuate the HPT-axis.

Cold exposure does not amplify the effect of DCL-KD on body weight and fat mass

Aside from regulating basal metabolic rate, thyroid hormones are important activators of thermogenesis in brown adipose tissue (BAT) and white adipose tissue (WAT)[23]. As such, we questioned whether the metabolic effects of DCL-KD might be enhanced by cold exposure, a condition that generally upregulates the HPT axis[24]. To test this, DCL-KD mice and WT littermates were investigated after five weeks of dox-containing diet. Consistent with our previous observations, DCL-KD mice gained less weight than their WT littermates (Fig. 3A), which was again explained by lowered fat mass (Fig. 3B). In this experiment, DCL-KD mice also showed a slight but significant lower lean mass compared to WT littermates (Fig. 3C). After the fifth week, the mice were individually housed in metabolic cages for an additional week during which the environmental temperature was either kept at 21 °C or lowered to 4 °C. Cold exposure led to a reduction in body weight and fat mass in both the DCL-KD and WT littermates, with no obvious interaction between genotype and temperature (Fig. 3D–F). Likewise, cold exposure increased energy expenditure (Fig. 4A, uncorrected data and corresponding VO_2 and VCO_2 data Supplementary Fig. S2A–E) and food intake (Fig. 4B), while reducing voluntary activity (Fig. 4C) independent of genotype. The cold-induced increase in energy expenditure was accompanied by a reduction in fat oxidation in the dark phase (Fig. 4D, uncorrected data Supplementary Fig. S3A), an overall increase in carbohydrate oxidation per gram lean mass (Fig. 4E, uncorrected data Supplementary Fig. S3B) as also reflected by a higher respiratory exchange ratio (Supplementary Fig. S3C). In line with the previous data, DCL-KD increased energy expenditure when expressed as per gram lean mass (according to two-way ANOVA genotype effect; Fig. 4A, uncorrected data and corresponding VO_2 and VCO_2 data Supplementary Fig. S2A–E), explained by increased fat oxidation in the light phase independent of cold exposure (Fig. 4D), while carbohydrate oxidation was unaffected by DCL-KD (Fig. 4E).

DCL-KD promotes browning of WAT

We next evaluated whether increased thermogenesis in BAT and/or WAT might contribute to the slightly increased energy expenditure and fat oxidation upon DCL-KD and whether these effects were independent of cold exposure as well. When thermogenic activity increases, BAT and/or WAT start taking up more triglyceride (TG)-derived fatty acids (FAs) from lipoproteins in the circulation for combustion. In order to study TG-derived FA uptake as an indication of thermogenic activity, mice were injected with TG-rich lipoprotein-like particles containing tri[^{3}H]oleate ([^{3}H]TO) at the end of the experiment. As expected, BAT was metabolically more active than WAT at 21 °C in WT as well as in DCL-KD mice and took up more TG-derived [^{3}H]oleate (approx. 10% of injected dose/g in BAT (Fig. 5A) vs < 1% of injected dose/g in WAT) (Fig. 5B), and cold exposure strongly increased [^{3}H]oleate uptake by BAT independent of genotype (Fig. 5A). Intriguingly, DCL-KD increased [^{3}H]oleate uptake by WAT (two-way ANOVA genotype effect, Fig. 5B), and this effect reached statistical significance in the post-hoc comparison of DCL-KD vs WT mice at 4 °C (Fig. 5B). Accordingly cold exposure led to a

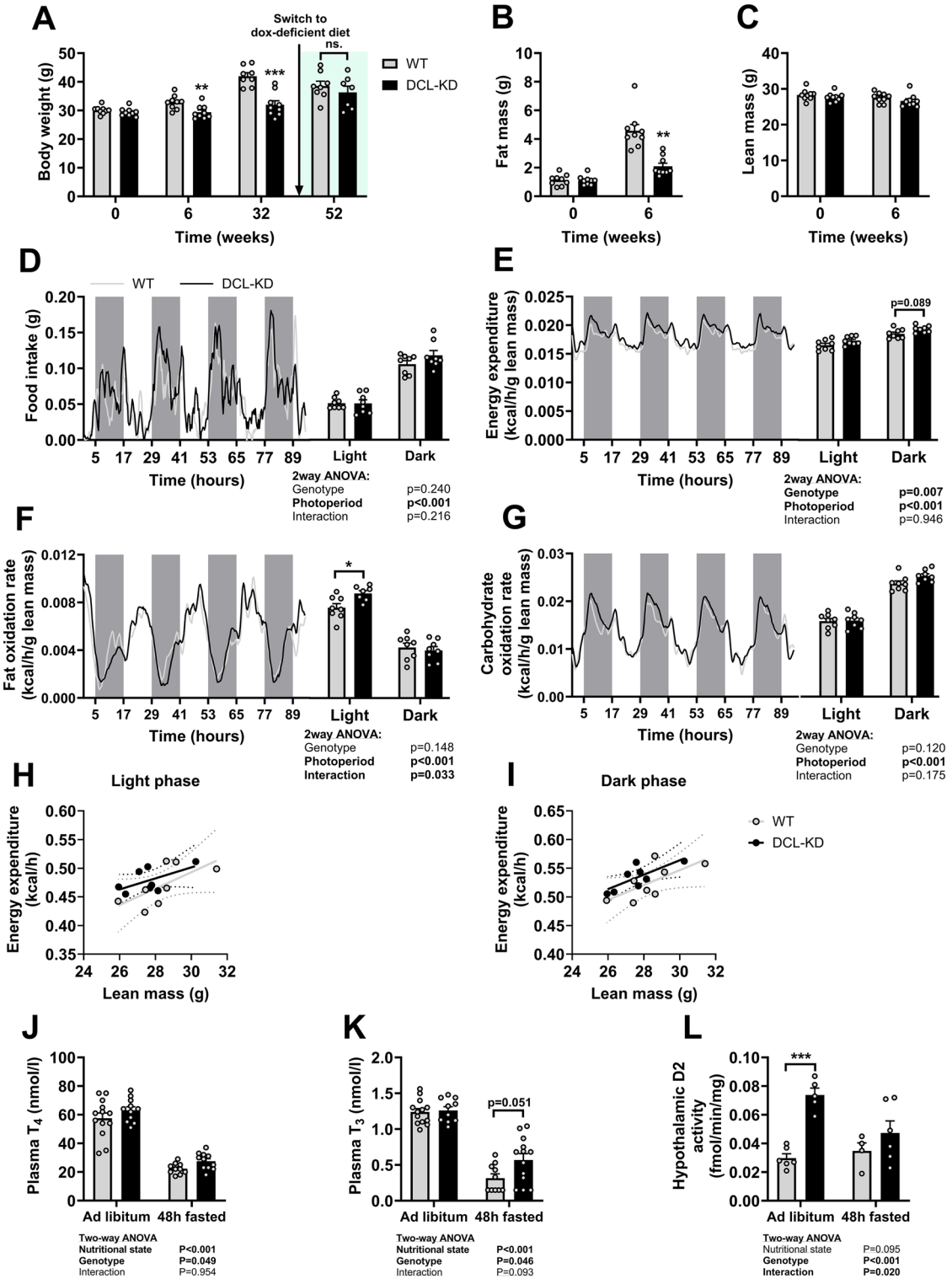

Fig. 2. DCL-KD prevents body weight gain in mice, due to lowered fat mass accumulation. DCL-KD mice (black bars) and WT littermates (grey bars) were fed a dox-containing diet for five weeks to induce DCL knockdown in the transgenic mice. (**A**) Body weight was monitored over a period of 52 weeks during which the dox-containing diet was replaced by dox-free diet at week 32. At week 0 and week 6 (**B**) fat mass and (**C**) lean mass were measured by Echo-MRI (n = 6–8 per group). In a separate study, mice were put on dox diet for 5 weeks. During the first 4 days mice were single-housed in metabolic cages while (**D**) food intake, and (**E**) energy expenditure (expressed per g lean mass), (**F**) fat oxidation rate, and (**G**) carbohydrate oxidation rate were monitored. (**H**,**I**) Energy expenditure was plotted against lean mass and linear regression was performed. At week 5, (**J**) plasma thyroxine, (**K**) plasma triiodothyronine, and (**L**) hypothalamic D2 activity were determined either in the ad libitum fed state or after 48 h of fasting (n = 5–8 per group). Data is presented as mean ± SEM. *P < 0.05, **P < 0.01, ***P < 0.001 according to unpaired t-test (**A**–**C**) or two-way ANOVA and following Šídák's multiple comparisons test (**E**–**G**,**J**–**L**).

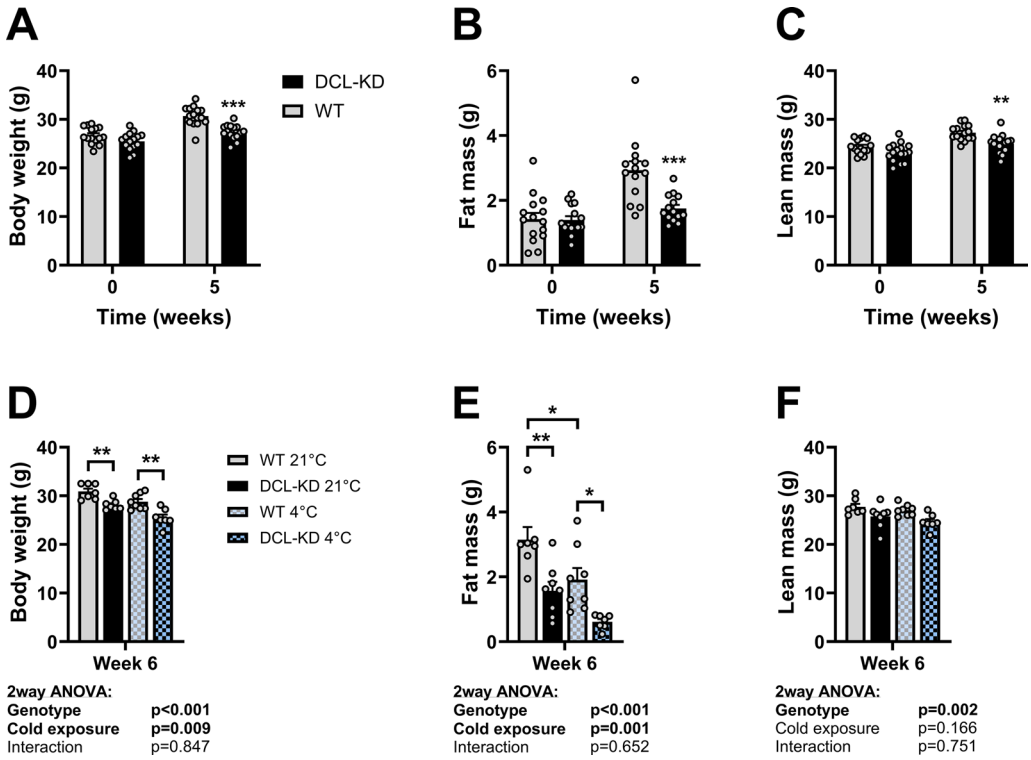

Fig. 3. DCL-KD and cold exposure additively reduce body weight and fat mass in mice. DCL-KD mice (black bars) and WT littermates (grey bars) were fed a dox-containing diet for five weeks to induce DCL knockdown in the transgenic mice. During week 6, mice were single-housed at 21 °C (solid) or 4 °C (blocked) for 1 week. At week 0, 5 and 6, (**A**,**D**) body weight, (**B**,**E**) fat mass (**C**,**F**) lean mass were determined [n = 16 per group for (**A**–**C**), and n = 8 per group for (**D**–**F**)]. Data is presented as mean ± SEM. *P < 0.05, **P < 0.01, ***P < 0.001 according to unpaired t-test (**A**–**C**) or two-way ANOVA and following Ŝídák's multiple comparisons test (**D**–**F**).

reduction in fasting plasma TG levels in DCL-KD but not WT mice (Fig. 5C). Circulating free fatty acid (FFA; Fig. 5D), glucose (Supplementary Fig. S3D) or insulin levels (Supplementary Fig. S3E) were not different between genotypes (Fig. 5D, Supplementary Fig. S3D).

We next evaluated other markers for thermogenic activity in BAT and WAT, including tissue weight, intracellular lipid content and UCP1 content, which is the critical enzyme for heat production in BAT[25]. Cold exposure reduced iBAT weight (Fig. 5E), tended to reduce sBAT weight (according to two-way ANOVA genotype effect Fig. 5E), and strongly lowered lipid content of iBAT (Fig. 5F) in line with increased thermogenic activity, while there was no effect of genotype on these parameters. In this experiment in lean mice, neither cold exposure, nor DCL-KD changed UCP1 protein content in BAT (Fig. 5G). In contrast to our findings in BAT, cold exposure and DCL-KD independently and additively lowered gWAT and sWAT weight (Fig. 5H), indicated by the two-way ANOVA genotype and cold exposure effects. DCL-KD also reduced sWAT cell size independent of cold exposure (Fig. 5I). In addition, four out of eight DCL-KD mice showed large UCP1 positive areas in their sWAT at 21 °C, while this was only the case for one of seven WT mice (Fig. 5J). *Ucp1* gene transcript could reliably be detected in six out of eight DCL-KD mice versus zero of the seven WT mice (not shown). Together with the increased TG-derived FA uptake by WAT, these data indicate that cold exposure and DCL-KD increase thermogenic activity in WAT.

To summarize, we show that DCL-KD does not affect BAT thermogenesis, but instead induces browning in WAT, which might contribute to the increased energy expenditure and weight loss.

Discussion

Hypothalamic tanycytes form important connections between the third ventricle, portal capillaries in the ME and multiple hypothalamic nuclei involved in regulation of energy homeostasis. In earlier work, we identified DCL to be highly expressed by β-tanycytes that line the third ventricle in the ME[14]. DCL expression has previously been linked to neurogenesis, but the role of DCL in β-tanycytes was still unknown[16,17]. Therefore, we studied the role of DCL in regulation of energy metabolism by using mice with inducible DCL knockdown after dox-administration in food pellets. In DCL-KD mice, we observed a strongly decreased DCL expression in hypothalamic tanycytes which was associated with less body weight gain on regular chow diet, explained by lowered fat mass gain, possibly as a result of browning of WAT.

DCL-KD KD resulted in prevention of body weight gain, which was in large explained by lower fat mass in DCL-KD mice versus WT littermates. These data are in line with previous reports showing that tanycytes are essential for body weight control, specifically demonstrating that pharmacological interference with or ablation

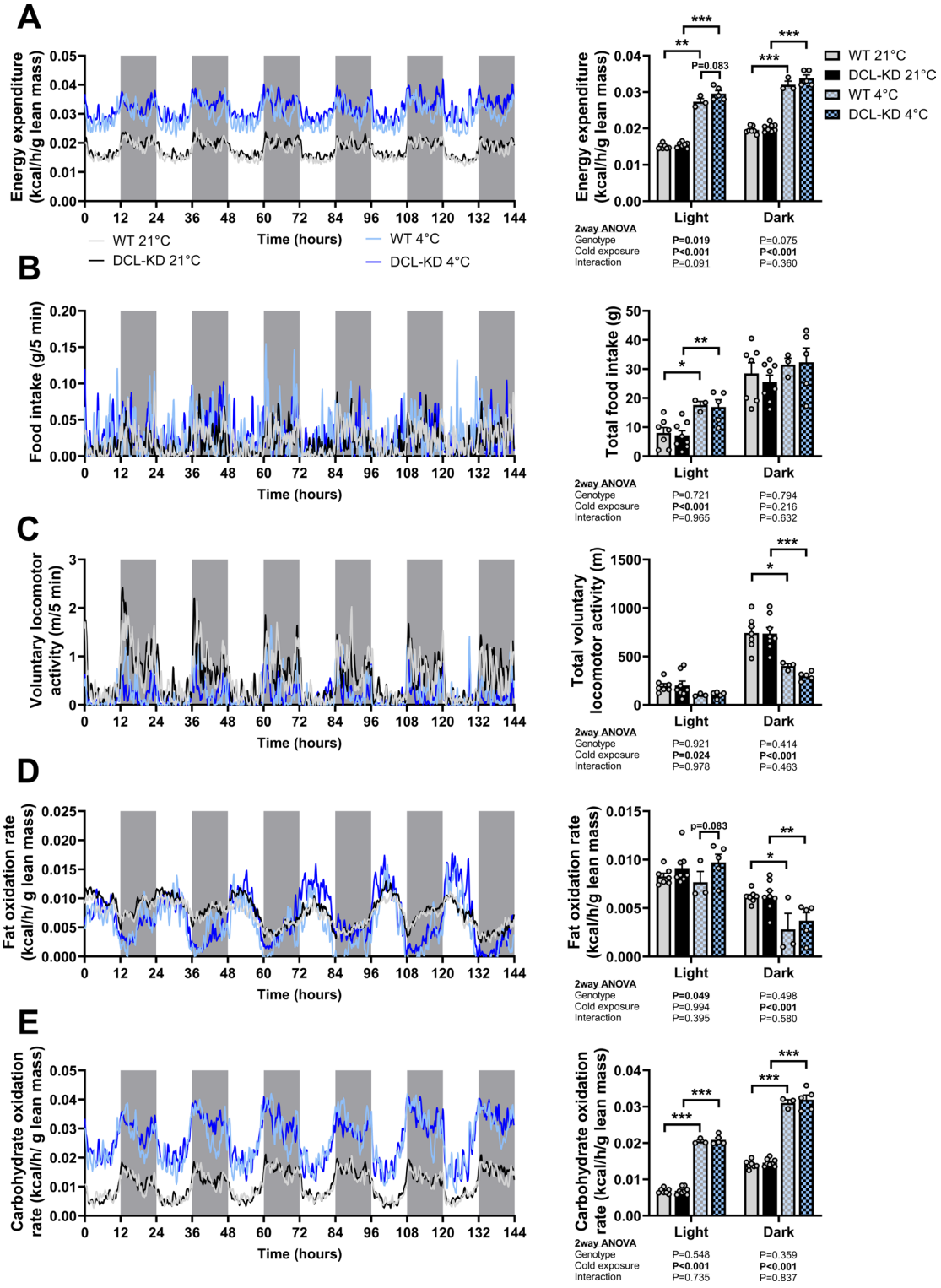

Fig. 4. DCL-KD increases energy expenditure and fat oxidation in mice. DCL-KD mice (black bars) and WT littermates (grey bars) were fed a dox-containing diet for five weeks to induce DCL knockdown in the transgenic mice. During week 6, mice were single-housed at 21 °C (solid) or 4 °C (blocked) in metabolic cages for 1 week while (**A**) energy expenditure, (**B**) food intake, (**C**) activity, (**D**) fat oxidation rate, and (**E**) carbohydrate oxidation rate were monitored (n = 3–8 per group). Values shown in (**A**), (**D**) and (**E**) are expressed per g lean mass. Bar graphs present means ± SEM. *P < 0.05, **P < 0.01, ***P < 0.001 according to two-way ANOVA and following Tukey's multiple comparisons test.

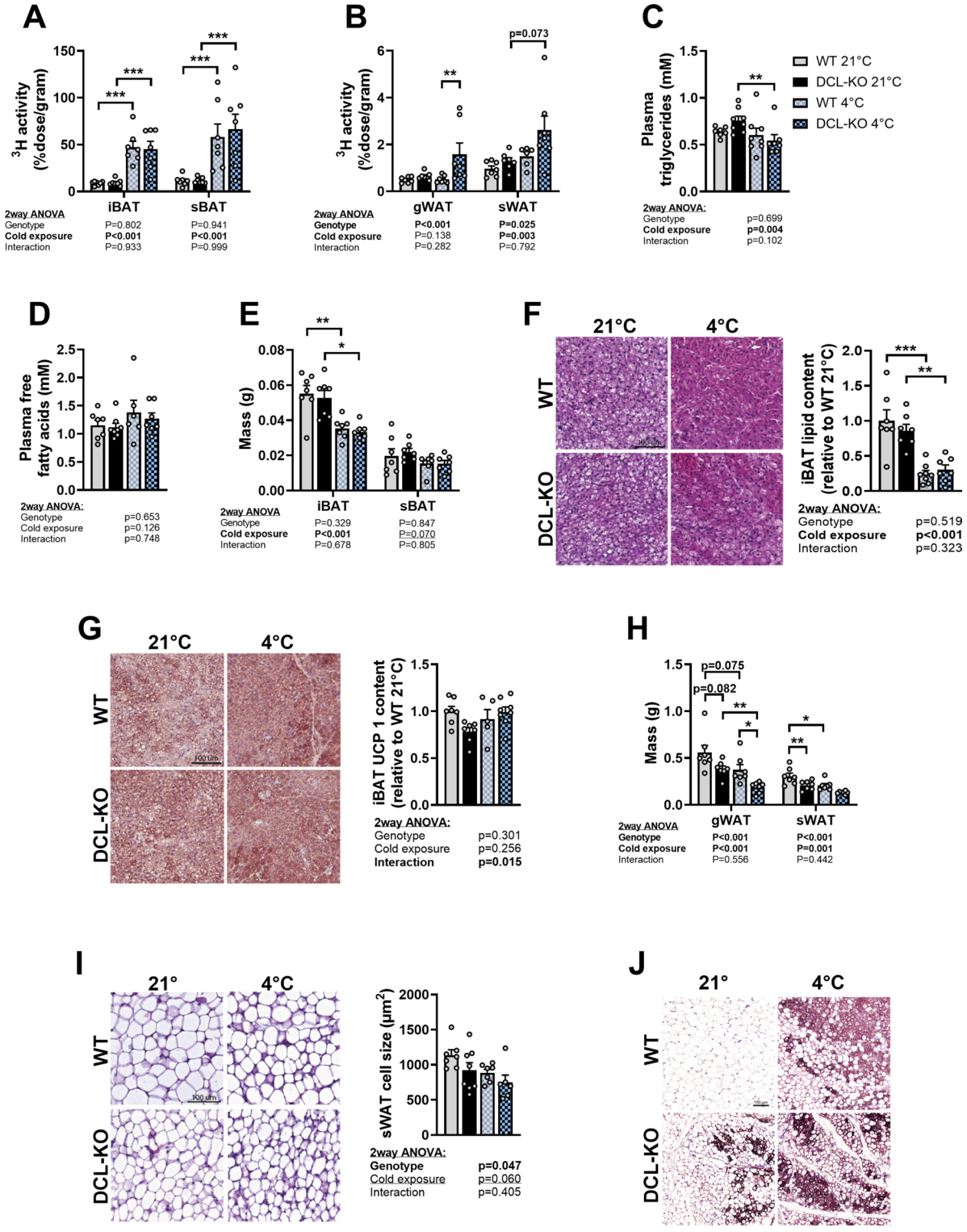

Fig. 5. DCL-KD lowers WAT cell size while increasing TG-derived FA uptake by the tissue. DCL-KD mice (black bars) and WT littermates (grey bars) were fed a dox-containing diet for 5 weeks to induce DCL knockdown in the transgenic mice. During week 6, mice were single-housed at 21 °C (solid) or 4 °C (blocked) after which the mice were injected with triglyceride-rich lipoprotein-like particles labeled with glycerol tri[3H]oleate to assess uptake of [3H] oleate by (**A**) interscapular brown adipose tissue (iBAT), subscapular BAT (sBAT) (**B**) gonadal white adipose tissue (gWAT) and subcutaneous WAT (sWAT). Plasma was collected before particle injection and levels of (**C**) triglycerides and (**D**) free fatty acids were measured. (**E**) iBAT, sBAT, (**F**) gWAT and sWAT depots were weighed. In iBAT, (**G**) lipid content and (**H**) uncoupling protein-1 (UCP-1) protein content were quantified after haematoxylin & eosin (H&E) staining and immunostaining, respectively. In sWAT, (**I**) adipocyte size and (**J**) UCP-1 protein content were determined by H&E staining and immunostaining, respectively (n = 7–8 per group). Data is presented as mean ± SEM. *P < 0.05, **P < 0.01, ***P < 0.001 according to two-way ANOVA (**A**,**B**,**D**–**I**) or two-way ANOVA on ranked values (**C**) and following Ŝídák's (**A**–**C**,**E**,**F**) or Tukey's (**D**,**E**,**G**) multiple comparisons test.

of tanycytes alters susceptibility to obesity in mice[18–20,26]. We additionally showed that the effect of DCL-KD on body weight gain is reversible and most likely explained by elevated energy expenditure, although we were not able to consistently demonstrate this throughout the various experiment due to the rather small effect size and relatively large variation between mice. Nonetheless, consistent with higher energy expenditure we did observe mildly elevated thyroid hormone levels upon DCL-KD. Mechanistically, hypothalamic tanycytes are thought to be part of a negative feedback mechanism controlling the set point of the HPT-axis[2,9]. As part of this negative feedback, tanycytes increase the size of their end-feet around the portal capillaries when TRH is released into the ME by hypophysiotropic neurons, thereby shielding pituitary vessels[9]. These kind of structural alterations require fast rearrangements of the microtubule and actin cytoskeleton. DCL has been described to control rapid adaptations of the cytoskeleton in neurogenesis and dendritic remodeling by controlling rapid adaptations of the cytoskeleton[16,27,28], which makes it very plausible that DCL is also involved in controlling tanycytic end-feet alterations. We anticipate that DCL deficiency impairs enlargement of tanycyte end-feet, thereby increasing the amount of TRH that the pituitary is exposed to, leading to more release of thyroid stimulating hormone (TSH) and subsequently T_4. Surprisingly, we observed increased hypothalamic D2-activity in DCL-KD. Since this enzyme is exclusively expressed by β-tanycytes in the hypothalamus, its increased activity would theoretically raise local T_3 levels, an effect that is known to downregulate TRH release and expression[2]. Nonetheless, this possible downregulation of TRH did not lead to lower T_4/T_3 levels in our DCL-KD mice.

In addition to increasing basal metabolic rate, thyroid hormone signaling is crucial for the regulation of adaptive thermogenesis[22]. Upon cold exposure, the sympathetic nervous system acutely stimulates thermogenesis in BAT, while T_3 is needed too for the activation of adaptive thermogenic programs[29,30]. For that reason, we tested whether the effect of cold would be more pronounced in the context of DCL-KD. In contrast to our expectations, we observed no interaction between genotype and environmental temperature in the control of BAT. An explanation for this might be that the mildly increased thyroid hormone levels after DCL-KD were insufficient to initiate the adaptive program in BAT. Alternatively, the use of lean mice, which already show rather high BAT activity at a temperature of 21 °C, might have prevented further activation of the tissue.

Most strikingly, we did observe clear signs of thermogenic activity in WAT of DCL-KD mice. Compared with their WT littermates, uptake of TG-derived FAs by WAT was increased while tissue weights were lower in DCL-KD mice. We confirmed this latter observation at histological levels, showing reduced adipocyte cell size, and a higher number UCP1 positive areas in WAT of DCL-KD than in WT mice. *Ucp1* transcript was also detected more often in WAT of DCL-KD than in WT mice. However, at group level there was large spread, and often very low expression brown adipocytes specific genes, possibly as a result of localized browning. Therefore those data could not be included in the current manuscript. Interestingly the effects of DCL-KD were found to be additive to the effects of cold exposure, suggestive of regulation through independent pathways. In line with this notion, a synthetic thyroid hormone receptor agonist was previously shown to upregulate expression of thermogenic genes, including *Ucp-1*, in WAT but not BAT[31]. The authors explained these effects by a direct effect of the agonist on white adipocytes, accompanied by a compensatory downregulation of sympathetic innervation of BAT.

Although DCL has a highly restrictive expression pattern in β-tanycytes[14], we cannot exclude the possibility that other brain areas are involved and the fact that we have been using a whole-body transgenic system to overexpress a shRNA against DCL represents a limitation of the current work. We have previously performed an extensive characterization of the neuronal cell populations expressing DCL[14]. Surrounding the third ventricle we demonstrated vimentin expression in both tanycytes and ependymal cells, while DCL was only expressed in tanycytes. Within the hypothalamus as a whole, DCL was also found to be expressed in the shell of the suprachiasmatic nucleus (SCN)[21]. However, the SCN is primarily implicated in the circadian aspects of the energy balance[32,33], a phenomenon that is not affected in our experiments (see Figs. 2, 4 and supplementary data). In addition we found DCL to be expressed in regions with suspected neurogenesis or neuronal plasticity, including the rostral migratory stream, olfactory bulb, and hippocampus. Neurogenesis in the adult hypothalamus has been implicated in feeding regulation as well[34]. Nevertheless, we did not observe difference in feeding behavior and we previously found no evidence for colocalization of DCL-positive cells with BrdU-positive cells in the hypothalamus (unpublished data). Therefore, together with the well-established role of β-tanycytes in the control of the energy balance, we favor the hypothesis that diminished DCL expression in these cells is causally related with the phenotype of DCL-KD mice.

The question remains how exactly DCL is involved in regulating tanycyte function. We already elaborated on the possibility of regulating the accessibility of pituitary vessels, but tanycytes can also control the degree of fenestration in the portal capillaries of the ME. Tanycytes can sense small declines in plasma glucose levels during fasting and respond by increasing the production of vascular endothelial growth factor (VEGF) that increases capillary permeability and induces reorganization of tanycytic tight junctions[35]. Interestingly, when this response is inhibited through Axitinib treatment, mice gain less weight during refeeding after 24 h of food deprivation[35]. In addition, tanycytes are known to actively shuttle hormones and metabolites between the circulation, CSF and hypothalamic nuclei. For example, the anorexigenic hormone leptin is taken up from portal capillaries by the tanycytic end-feet and is subsequently intracellularly transported via clathrin-coated vesicles to the CSF[5,6]. In addition to leptin, recent studies demonstrated that the appetite-inducing hormone ghrelin[36,37] and possibly also glucagon-like peptide 1 (GLP-1)[38,39] are transported by tanycytes. Intriguingly, DCLK1, of which DCL is a splice-variant, has been implicated in kinesin-mediated cargo transport[40], making the idea that tanycytes in DCL-KD mice have altered transportation capacities an attractive hypothesis. Considering that transfer of leptin into the brain by tanycytes is reduced in obese individuals and in diet-induced obese mice[6,41,42], targeting DCL in obesity might be an interesting therapeutic option.

In summary, we show an important role of tanycytic DCL in body weight control through regulation of thyroid hormone release, energy expenditure, and specifically WAT browning, in mice. Elucidating the mechanisms

underlying the role of DCL in regulating brain-peripheral crosstalk further might identify new treatment targets for obesity.

Methods

Animals

Male transgenic mice that contain an inducible and reversible shRNA expression system were originally obtained from Taconic Artemis (Cologne, Germany). Sequences targeting DCL were cloned into the shRNA expression system as described by others[43]. We have described the generation of these DCL-KD mice in detail elsewhere, and studied the implication of DCL-knockdown for hippocampal neurogenesis[17]. These animals were maintained at the Leiden University Medical Center as an outbred colony and were used for all experiments used in this article. The animals were kept under standard conditions in a 12:12 h light–dark cycle with ad libitum access to water and food unless stated otherwise. Researchers were blinded for genotype during the experiments, cages were placed in random order, and mice were handled in random order to avoid bias or confounding. The shRNA system was induced via dox-containing food pellets (Dox Diet Sterile S3888, 200 mg/kg, BioServ, New Jersey, USA).

In experiment 1, 6 week-old male DCL-KD and WT littermates (n = 6 mice per group) were fed a dox-containing diet for five weeks before the animals were deeply anaesthetized by intraperitoneal injection of sodium pentobarbital. Thereafter the mice were transcardially perfused with ice-cold 0.1 M phosphate-buffered saline (PBS) and subsequently with 4% paraformaldehyde (PFA) in 0.1 M PBS. After perfusion, the mice were killed by decapitation and the heads kept in 4% PFA overnight at 4 °C for post fixation.

In experiment 2, 12 week-old male DCL-KD and WT littermates (n = 9 mice per group) were fed a dox-containing diet for 32 weeks, after which the diet was switched to a dox-free diet for another 20 weeks. Body weight was monitored regularly, and lean and fat body mass were determined in week 0 and 6 (EchoMRI 100-Analyzer; EchoMRI, Houston, Texas). At the end of the experiment the mice were killed by CO_2 suffocation.

In experiment 3, 12 week-old male DCL-KD and WT littermates (n = 8 mice per group) were fed a dox-containing diet for 5 weeks, and mice were single-housed during the first 4 days while energy expenditure was monitored via indirect calorimetry. At week 5, mice were fasted for 48 h for assessment of serum T_4 and T_3 levels. Subsequently, mice were killed by CO_2 suffocation and the hypothalamus (defined rostrally by the optic chiasm, caudally by the mamillary bodies, laterally by the optic tract, and dorsally by the apex of the third ventricle) was isolated and stored immediately in liquid nitrogen.

In experiment 4, 12 week-old male DCL-KD and WT littermates (n = 16 mice per group) were fed a dox-containing diet for 5 weeks, after which the mice were single-housed at 21 °C (n = 8 mice per genotype) or 4 °C (n = 8 mice per genotype) for 8 additional days while energy expenditure was monitored via indirect calorimetry. At the end of the experiment, mice were fasted for 4 h before assessing plasma lipid, glucose and insulin levels, and intravenous injection of TG-rich lipoprotein-like particles. Fifteen minutes after the injection, the mice were killed by CO_2 suffocation to assess organ distribution. Additional pieces of organs and tissues were collected for further histological assessment.

All animal experiments were approved by the Central Authority for Scientific Procedures on Animals (CCD) of the Netherlands and by the Ethics Committee on Animal Care and Experimentation of the Leiden University Medical Center, The Netherlands. All work with animals was performed in accordance with the Dutch Act on Animal Experimentation and EU Directive 2010/63/EU. The study is reported in accordance with ARRIVE guidelines.

Antibodies and immunofluorescent staining

Subsequent to overnight fixation in 4% PFA after collection, brains were put in a 15% sucrose solution (0.1 M PBS) overnight at 4 °C for dehydration followed by a 30% sucrose solution for another night at 4 °C. At the end of the dehydration procedure the brains were removed from the solution and blotted dry before snap-freezing. The brains were kept at – 80 °C until used for cryosectioning. Serial coronal 30 µm-thick sections were obtained using a cryostat. All brain sections were collected in anti-freeze (50% glycerol, 50% 0.2 M PBS) and stored at – 20 °C until further use. Free floating sections were left at room temperature for 15 min before being washed in 0.1 M PBS and blocked in 2% bovine serum albumin (BSA, sc-2323, Santa Cruz Biotechnology, Dallas, USA) in PBS for 2 h. After three washing steps in PBS the primary antibody targeting DCL (1:1000, homemade and described in detail earlier)[14] was applied to the slides in PBS with 0.3% Triton X-100 and left at room temperature for 1 h followed up by overnight incubation at 4 °C. Subsequently the slides were washed in PBS and incubated in secondary antibody (Alexa Fluor® 488 donkey anti-rabbit IgG, Thermo-Fisher, Waltham, USA) for 2 h at room temperature. After washing with PBS the slides were counterstained with Hoechst (1:10,000) for 10 min and washed again before they were mounted and covered using Aqua Poly/Mount (Polysciences, Inc., Warrington, UK).

Serum T_4 and T_3 levels

Serum T_4 and T_3 were measured with in-house radio immunoassays as described before[44,45]. All samples of one experiment were measured within the same run.

Indirect calorimetry

Indirect calorimetry was carried out in metabolic home-cages (LabMaster System, TSE Systems, Bad Homburg, Germany for experiment 3; Promethion line, Sable Systems International, Las Vegas, NV, USA for experiment 4). Mice were single housed and data collection started after two days of acclimatization. Specifically, food intake, O_2 consumption (mL/h), and CO_2 production (mL/h) were recorded, from which energy expenditure, fat oxidation rate, and carbohydrate oxidation rate were calculated[46]. Data are shown as whole-body oxidation

rates and expressed per g lean mass. Linear regression was performed to assess oxidation as function of body weight and lean mass.

D2 activity assay

The isolated hypothalamic block was homogenized on ice in PED50 (0.1 M sodium phosphate, 2 mM EDTA and 50 mM DTT pH 7.2) using a Polytron (Kinematica, Luzern, Switzerland). Homogenates were immediately processed for D2 measurement in duplicate as previously described[47]. Protein concentration was measured with the Bio-Rad protein assay using BSA as the standard following the manufacturer's instructions (Bio-Rad Laboratories, Veenendaal, The Netherlands). Samples were incubated for 4 h, at 37 °C with 1 or 500 nM T_4, 500 nM 6n-propylthiouracil (to block D1) and 2×10^5 cpm [3′5′-(125)I]T_4. The reaction was stopped by cooling the samples on ice and adding ice-cold ethanol (1:1 ratio). After centrifugation, the supernatant was mixed with 0.02 M ammonium acetate (pH 4; 1:1 ratio), and 100 µL of the mixture was applied to 4.6 × 250 mm Symmetry C18 column connected to a Waters HPLC system (Model 600E pump, Model 717 WISP autosampler, Waters, EttenLeur, The Netherlands). Mobile phase A: 0.02 M ammonium acetate (pH 4.0), mobile phase B: acetonitrile. The column was eluted with a linear gradient (28–42% B in 15 min) at a flow of 1200 µL/min. The activity of T4, and T3 in the eluate was measured online using a FSA flow detector (150TR, PerkinElmer, Groningen, The Netherlands). D2 activity was expressed as fmol of generated T_3 per minute per mg of tissue. The amount of generated T_3 was calculated using the values of the 1 nM T_4 incubations minus the mean of the 500 nM T_4 incubations.

In vivo organ uptake of TG-derived FAs

TG-rich lipoprotein-like particles labeled with glycerol tri[^{3}H]oleate were prepared as described before[48]. Particles were injected into the tail vein (1 mg triglycerides (TG) per mouse in 200 µL saline) 15 min before the mice were killed. Subsequently, mice were perfused transcardially with ice-cold PBS for 5 min before various (parts of) organs (approximately 50–150 mg) were collected and dissolved in 0.5 mL Solvable (6NE9100, PerkinElmer, Waltham, USA) at 56 °C overnight, after which 5.0 mL Ultima Gold (6013329, PerkinElmer, Waltham, USA) was added. ^{3}H-activity was measured with a scintillation counter (Tri-Carb 2910 TR, PerkinElmer, Waltham, USA) and expressed as a percentage of the injected dose per gram tissue.

Plasma measurements

To determine TG, FFA and glucose levels, colorimetric measurements were performed using commercially available kits (Roche Diagnostics, Mannheim, Germany). Insulin levels were determined by using an Ultra Sensitive Mouse Insulin ELISA Kit (90080, Crystal Chem, Zaandam, Netherlands).

Adipose tissue histology

Formalin-fixed paraffin-embedded interscapular brown adipose tissue (iBAT) and subcutaneous white adipose tissue (sWAT) tissue sections (5 µm) were prepared for haematoxylin and eosin staining using standard protocols, and uncoupling protein-1 (UCP-1) immunostaining as described previously[49]. The areas occupied by intracellular lipid vacuoles and UCP-1 protein within the iBAT were quantified using Image J software (version 1.52a; National Institutes of Health, Bethesda, Maryland). To measure white adipocyte size the function "analyze particles" was used in Image J with criteria of size between 40 and 1800 pixels and a circularity of at least 0.10.

Statistical analysis

In case of data that was measured at multiple timepoints, two-way ANOVA with post-hoc Šídák's test was performed to compare WT and DCL-KD mice over time. In case of measurements that were taken in two different conditions (e.g., fasted versus fed conditions, or 21 °C versus 4 °C), two-way ANOVA was used to calculated the main effect of the genotype, main effect of the condition and the interaction effect, while all separate groups were compared to each other using post-hoc Šídák's or Tukey's test. For purpose of readability of the graphs, only comparisons between genotypes in the same condition, or between conditions within the same genotype are shown. All data was tested for normality and, in case of non-normal distribution, two-way ANOVA was performed on ranked values. Statistical outliers were removed using Grubb's test. Statistical analyses were performed with GraphPad Prism software, version 9.3.1 (GraphPad, La Jolla, California). $P < 0.05$ was considered statistically significant and data are presented as means ± SEM.

Data availability

The data that support the findings of this study are available in the Materials and Methods, Results, and/or Supplemental Material of this article.

Received: 24 April 2024; Accepted: 20 August 2024
Published online: 22 August 2024

References

1. Schneeberger, M., Gomis, R. & Claret, M. Hypothalamic and brainstem neuronal circuits controlling homeostatic energy balance. *J. Endocrinol.* **220**, T25-46. https://doi.org/10.1530/joe-13-0398 (2014).
2. Rodríguez-Rodríguez, A. *et al.* Tanycytes and the control of thyrotropin-releasing hormone flux into portal capillaries. *Front. Endocrinol. (Lausanne)* **10**, 401. https://doi.org/10.3389/fendo.2019.00401 (2019).
3. Rizzoti, K. & Lovell-Badge, R. Pivotal role of median eminence tanycytes for hypothalamic function and neurogenesis. *Mol. Cell Endocrinol.* **445**, 7–13. https://doi.org/10.1016/j.mce.2016.08.020 (2017).

4. Imbernon, M. *et al.* Tanycytes control hypothalamic liraglutide uptake and its anti-obesity actions. *Cell Metab.* **34**, 1054-1063. e1057. https://doi.org/10.1016/j.cmet.2022.06.002 (2022).
5. Duquenne, M. *et al.* Leptin brain entry via a tanycytic LepR-EGFR shuttle controls lipid metabolism and pancreas function. *Nat. Metab.* **3**, 1071–1090. https://doi.org/10.1038/s42255-021-00432-5 (2021).
6. Balland, E. *et al.* Hypothalamic tanycytes are an ERK-gated conduit for leptin into the brain. *Cell Metab.* **19**, 293–301. https://doi.org/10.1016/j.cmet.2013.12.015 (2014).
7. Elizondo-Vega, R. *et al.* The role of tanycytes in hypothalamic glucosensing. *J. Cell Mol. Med.* **19**, 1471–1482. https://doi.org/10.1111/jcmm.12590 (2015).
8. Langlet, F. Tanycytes: A gateway to the metabolic hypothalamus. *J. Neuroendocrinol.* **26**, 753–760. https://doi.org/10.1111/jne.12191 (2014).
9. Müller-Fielitz, H. *et al.* Tanycytes control the hormonal output of the hypothalamic–pituitary–thyroid axis. *Nat. Commun.* **8**, 484. https://doi.org/10.1038/s41467-017-00604-6 (2017).
10. Kovari, D. *et al.* Tanycyte specific ablation of diacylglycerol lipase alpha stimulates the hypothalamic–pituitary–thyroid axis by decreasing the endocannabinoid mediated inhibition of TRH release. *J. Neuroendocrinol.* **34**, e13079. https://doi.org/10.1111/jne.13079 (2022).
11. Tu, H. M. *et al.* Regional distribution of type 2 thyroxine deiodinase messenger ribonucleic acid in rat hypothalamus and pituitary and its regulation by thyroid hormone. *Endocrinology* **138**, 3359–3368. https://doi.org/10.1210/endo.138.8.5318 (1997).
12. Fekete, C. *et al.* DARPP-32 and CREB are present in type 2 iodothyronine deiodinase-producing tanycytes: Implications for the regulation of type 2 deiodinase activity. *Brain Res.* **862**, 154–161. https://doi.org/10.1016/s0006-8993(00)02105-3 (2000).
13. Rodríguez, E. M. *et al.* Hypothalamic tanycytes: A key component of brain–endocrine interaction. *Int. Rev. Cytol.* **247**, 89–164. https://doi.org/10.1016/s0074-7696(05)47003-5 (2005).
14. Saaltink, D. J., Håvik, B., Verissimo, C. S., Lucassen, P. J. & Vreugdenhil, E. Doublecortin and doublecortin-like are expressed in overlapping and non-overlapping neuronal cell population: Implications for neurogenesis. *J. Comp. Neurol.* **520**, 2805–2823. https://doi.org/10.1002/cne.23144 (2012).
15. Schaar, B. T., Kinoshita, K. & McConnell, S. K. Doublecortin microtubule affinity is regulated by a balance of kinase and phosphatase activity at the leading edge of migrating neurons. *Neuron* **41**, 203–213. https://doi.org/10.1016/s0896-6273(03)00843-2 (2004).
16. Vreugdenhil, E. *et al.* Doublecortin-like, a microtubule-associated protein expressed in radial glia, is crucial for neuronal precursor division and radial process stability. *Eur. J. Neurosci.* **25**, 635–648. https://doi.org/10.1111/j.1460-9568.2007.05318.x (2007).
17. Saaltink, D. J., van Zwet, E. W. & Vreugdenhil, E. Doublecortin-like is implicated in adult hippocampal neurogenesis and in motivational aspects to escape from an aversive environment in male mice. *eNeuro.* https://doi.org/10.1523/eneuro.0324-19.2020 (2020).
18. Rohrbach, A. *et al.* Ablation of glucokinase-expressing tanycytes impacts energy balance and increases adiposity in mice. *Mol. Metab.* **53**, 101311. https://doi.org/10.1016/j.molmet.2021.101311 (2021).
19. Kim, S. *et al.* Tanycytic TSPO inhibition induces lipophagy to regulate lipid metabolism and improve energy balance. *Autophagy* **16**, 1200–1220. https://doi.org/10.1080/15548627.2019.1659616 (2020).
20. Yoo, S. *et al.* Tanycyte ablation in the arcuate nucleus and median eminence increases obesity susceptibility by increasing body fat content in male mice. *Glia* **68**, 1987–2000. https://doi.org/10.1002/glia.23817 (2020).
21. Coomans, C. *et al.* Doublecortin-like expressing astrocytes of the suprachiasmatic nucleus are implicated in the biosynthesis of vasopressin and influences circadian rhythms. *Glia* **69**, 2752–2766. https://doi.org/10.1002/glia.24069 (2021).
22. Mullur, R., Liu, Y. Y. & Brent, G. A. Thyroid hormone regulation of metabolism. *Physiol. Rev.* **94**, 355–382. https://doi.org/10.1152/physrev.00030.2013 (2014).
23. de Jesus, L. A. *et al.* The type 2 iodothyronine deiodinase is essential for adaptive thermogenesis in brown adipose tissue. *J. Clin. Investig.* **108**, 1379–1385. https://doi.org/10.1172/jci13803 (2001).
24. Zhang, Z., Boelen, A., Kalsbeek, A. & Fliers, E. TRH neurons and thyroid hormone coordinate the hypothalamic response to cold. *Eur. Thyroid J.* **7**, 279–288. https://doi.org/10.1159/000493976 (2018).
25. Ricquier, D. Uncoupling protein 1 of brown adipocytes, the only uncoupler: A historical perspective. *Front. Endocrinol. (Lausanne)* **2**, 85. https://doi.org/10.3389/fendo.2011.00085 (2011).
26. Sanders, N. M., Dunn-Meynell, A. A. & Levin, B. E. Third ventricular alloxan reversibly impairs glucose counterregulatory responses. *Diabetes* **53**, 1230–1236. https://doi.org/10.2337/diabetes.53.5.1230 (2004).
27. Shin, E. *et al.* Doublecortin-like kinase enhances dendritic remodelling and negatively regulates synapse maturation. *Nat. Commun.* **4**, 1440. https://doi.org/10.1038/ncomms2443 (2013).
28. Koizumi, H., Tanaka, T. & Gleeson, J. G. Doublecortin-like kinase functions with doublecortin to mediate fiber tract decussation and neuronal migration. *Neuron* **49**, 55–66. https://doi.org/10.1016/j.neuron.2005.10.040 (2006).
29. Zekri, Y. *et al.* Brown adipocytes local response to thyroid hormone is required for adaptive thermogenesis in adult male mice. *Elife.* https://doi.org/10.7554/eLife.81996 (2022).
30. Broeders, E. P. *et al.* Thyroid hormone activates brown adipose tissue and increases non-shivering thermogenesis—A cohort study in a group of thyroid carcinoma patients. *PLoS One* **11**, e0145049. https://doi.org/10.1371/journal.pone.0145049 (2016).
31. Lin, J. Z. *et al.* Pharmacological activation of thyroid hormone receptors elicits a functional conversion of white to brown fat. *Cell Rep.* **13**, 1528–1537. https://doi.org/10.1016/j.celrep.2015.10.022 (2015).
32. Kalsbeek, A. *et al.* Circadian disruption and SCN control of energy metabolism. *FEBS Lett.* **585**, 1412–1426. https://doi.org/10.1016/j.febslet.2011.03.021 (2011).
33. Hastings, M. H., Maywood, E. S. & Brancaccio, M. Generation of circadian rhythms in the suprachiasmatic nucleus. *Nat. Rev. Neurosci.* **19**, 453–469. https://doi.org/10.1038/s41583-018-0026-z (2018).
34. Sousa-Ferreira, L., de Almeida, L. P. & Cavadas, C. Role of hypothalamic neurogenesis in feeding regulation. *Trends Endocrinol. Metab.* **25**, 80–88. https://doi.org/10.1016/j.tem.2013.10.005 (2014).
35. Langlet, F. *et al.* Tanycytic VEGF-A boosts blood-hypothalamus barrier plasticity and access of metabolic signals to the arcuate nucleus in response to fasting. *Cell Metab.* **17**, 607–617. https://doi.org/10.1016/j.cmet.2013.03.004 (2013).
36. Cabral, A., Valdivia, S., Fernandez, G., Reynaldo, M. & Perello, M. Divergent neuronal circuitries underlying acute orexigenic effects of peripheral or central ghrelin: Critical role of brain accessibility. *J. Neuroendocrinol.* **26**, 542–554. https://doi.org/10.1111/jne.12168 (2014).
37. Collden, G. *et al.* Neonatal overnutrition causes early alterations in the central response to peripheral ghrelin. *Mol. Metab.* **4**, 15–24. https://doi.org/10.1016/j.molmet.2014.10.003 (2015).
38. Shirazi, R. *et al.* Glucagon-like peptide 1 receptor induced suppression of food intake, and body weight is mediated by central IL-1 and IL-6. *Proc. Natl. Acad. Sci. U. S. A.* **110**, 16199–16204. https://doi.org/10.1073/pnas.1306799110 (2013).
39. Secher, A. *et al.* The arcuate nucleus mediates GLP-1 receptor agonist liraglutide-dependent weight loss. *J. Clin. Investig.* **124**, 4473–4488. https://doi.org/10.1172/JCI75276 (2014).
40. Lipka, J., Kapitein, L. C., Jaworski, J. & Hoogenraad, C. C. Microtubule-binding protein doublecortin-like kinase 1 (DCLK1) guides kinesin-3-mediated cargo transport to dendrites. *Embo J.* **35**, 302–318. https://doi.org/10.15252/embj.201592929 (2016).
41. Caro, J. F. *et al.* Decreased cerebrospinal-fluid/serum leptin ratio in obesity: A possible mechanism for leptin resistance. *Lancet* **348**, 159–161. https://doi.org/10.1016/s0140-6736(96)03173-x (1996).

42. Schwartz, M. W., Peskind, E., Raskind, M., Boyko, E. J. & Porte, D. Jr. Cerebrospinal fluid leptin levels: Relationship to plasma levels and to adiposity in humans. *Nat. Med.* **2**, 589–593. https://doi.org/10.1038/nm0596-589 (1996).
43. Seibler, J. *et al.* Reversible gene knockdown in mice using a tight, inducible shRNA expression system. *Nucleic Acids Res.* **35**, e54. https://doi.org/10.1093/nar/gkm122 (2007).
44. Boelen, A. *et al.* Simultaneous changes in central and peripheral components of the hypothalamus–pituitary–thyroid axis in lipopolysaccharide-induced acute illness in mice. *J. Endocrinol.* **182**, 315–323. https://doi.org/10.1677/joe.0.1820315 (2004).
45. Wiersinga, W. M. & Chopra, I. J. Radioimmunoassay of thyroxine (T4), 3,5,3'-triiodothyronine (T3), 3,3',5'-triiodothyronine (reverse T3, rT3), and 3,3'-diiodothyronine (T2). *Methods Enzymol.* **84**, 272–303. https://doi.org/10.1016/0076-6879(82)84024-x (1982).
46. Berbée, J. F. *et al.* Brown fat activation reduces hypercholesterolaemia and protects from atherosclerosis development. *Nat. Commun.* **6**, 6356. https://doi.org/10.1038/ncomms7356 (2015).
47. Kwakkel, J. *et al.* Skeletal muscle deiodinase type 2 regulation during illness in mice. *J. Endocrinol.* **203**, 263–270. https://doi.org/10.1677/joe-09-0118 (2009).
48. Ying, Z., Boon, M. R., Coskun, T., Kooijman, S. & Rensen, P. C. A simplified procedure to trace triglyceride-rich lipoprotein metabolism in vivo. *Physiol. Rep.* **9**, e14820 (2021).
49. Kooijman, S. *et al.* Central GLP-1 receptor signalling accelerates plasma clearance of triacylglycerol and glucose by activating brown adipose tissue in mice. *Diabetologia* **58**, 2637–2646. https://doi.org/10.1007/s00125-015-3727-0 (2015).

Author contributions

M. Modder, P.C.N. Rensen, E. Vreugdenhil and S. Kooijman conceived and designed the research; M. Modder, C.P. Coomans, D. Saaltink, M. Tersteeg, J. Hoogduin , L. Scholten, A.C.M. Pronk, R.A. Lalai, A. Boelen, and A. Kalsbeek performed the research and acquired the data; M.Modder, P.C.N. Rensen, E. Vreugdenhil and S. Kooijman analyzed and interpreted the data. All authors were involved in drafting and revising the manuscript.

Competing interests

The authors declare no competing interests.

Additional information

Supplementary Information The online version contains supplementary material available at https://doi.org/10.1038/s41598-024-70639-5.

Correspondence and requests for materials should be addressed to S.K.

Reprints and permissions information is available at www.nature.com/reprints.

Publisher's note Springer Nature remains neutral with regard to jurisdictional claims in published maps and institutional affiliations.